ChemComm

Accepted Manuscript

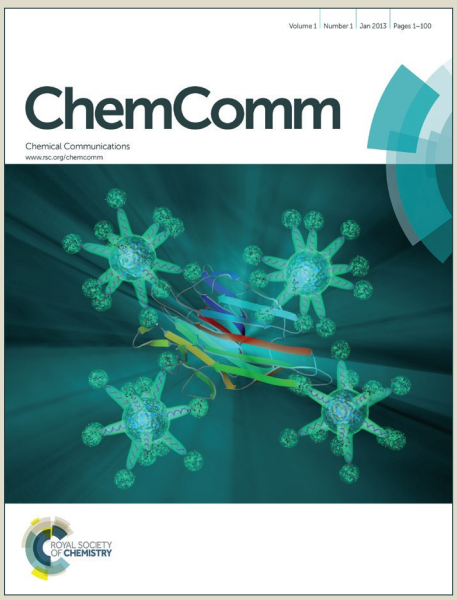

ROYAL SOCIETY OF CHEMISTRY

www.rsc.org/chemcomm

Chem. Commun.

RSCPublishing

COMMUNICATION

Bio-inspired Multinuclear Copper Complexes Covalently Immobilized on Reduced Graphene Oxide as Efficient Electrocatalysts for the Oxygen Reduction Reaction

Cite this: DOI: 10.1039/xoxxoooooox

Received ooth January 2012,
Accepted ooth January 2012

DOI: 10.1039/xoxxoooooox

Yue-Ting Xi,[a] Ping-Jie Wei,[a] Ru-Chun Wang,[a] and Jin-Gang Liu*[a]

Inspired by the multicopper active site of laccase, which efficiently catalyzes the oxygen reduction reaction (ORR), herein we report a novel bio-inspired ORR catalyst composed of a multinuclear copper complex that was immobilized on the surface of reduced graphene oxide (rGO) via the covalent grafted triazole-dipyridine (TADPy) dinucleating ligand. This rGO-TADPyCu catalyst exhibited high ORR activity, and superior long-term stability to Pt/C in alkaline media.

The lack of availability of efficient cathodic oxygen reduction reaction (ORR) catalysts is the major barrier to the large-scale commercialization of low-temperature fuel cells.[1] Currently, the noble-metal platinum (Pt) and its alloys are predominantly used as the ORR catalysts in low-temperature fuel cells such as hydrogen/air polymer electrolyte fuel cells, direct methanol fuel cells, and metal-air batteries.[2] However, the sluggish ORR at the cathode generally requires a higher loading of Pt on the cathode.[2] The disadvantages of high cost and scarce reserves together with a low tolerance to fuel crossover of Pt-based catalysts mean that developing low-cost, non-precious-metal catalysts for ORR is of paramount importance for the large commercial fuel cell market. The non-precious-metal catalysts have been extensively pursued mainly through the traditional method of pyrolysis of various precursors, including transition metal complexes of nitrogen-containing precursors, transition metal oxides, and chalcogenides, as well as metal-organic frameworks.[2-5] This pyrolysis approach largely depends on trial-and-error-based experiments for optimizing the ORR activity, while the actual nature of the active sites remains a subject of debate.

On the other hand, ORR catalysts prepared in a non-pyrolyzed manner have attracted interest because they provide the ability to adequately control the ORR catalyst structure and the underlying support material, thus fine tuning the ORR activity in a structure-function controllable way.[6] In addition, the design of new ORR catalysts using a biomimetic approach could benefit from the relatively clean O_2 activation/reduction mechanisms, and thus high efficiency of the enzymatic catalytic reactions.[7, 8] For instance, taking inspiration from the naturally occurring oxygen activation/reduction metalloenzymes such as the heme-containing enzymes, we have reported a biomimetic ORR electrocatalyst, an axial imidazole-coordinated porphyrin covalently grafted to multi-walled carbon nanotubes, which showed remarkable and superior ORR activity and stability compared to commercial Pt/C catalysts in both acidic and alkaline environments.[7a]

Copper ions have been implicated in various copper enzymes for O_2-binding, activation, and reduction.[9, 10] The multicopper oxidase enzymes, such as laccase, very efficiently catalyze the four-electron reduction of O_2 to H_2O with very low overpotential, where the active center features in a tri-copper O_2-binding/reduction site (Figure 1a).[10] For their biological relevance, numerous Cu complexes including multinuclear Cu compounds have been explored as ORR catalysts, although most of the systems exhibited relatively low ORR activity as well as poor catalyst stability.[11-13] Among all those reported copper complexes, the most efficient Cu-complex-based ORR electrocatalyst is a triazole copper compound [Cu(Hdatrz)], with an ORR onset potential of 0.86 V (vs. RHE) at pH 13.[11a] However, the long-term stability of the [Cu(Hdatrz)] catalyst is poor, and it degrades substantially over repeat potential cycles in alkaline media.[11b]

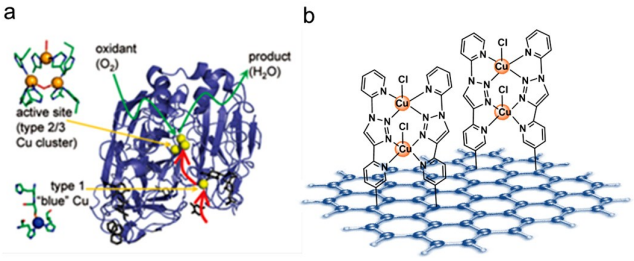

Figure 1 (a) Schematic representation of the multicopper active site in laccase and its catalytic reduction of oxygen to water.[10b] (b) Schematic representation of the bio-inspired multicopper complexes covalently anchored to the surface of reduced graphene oxide, rGO-TADPyCu, as an ORR electrocatalyst.

Recent ORR studies of mononuclear Cu complexes covalently immobilized on the surface of glassy carbon have suggested that two proximal coordinated Cu^I sites are required for efficient O_2 reduction, and a Cu polynuclear assembly is the key to attaining four-electron reduction of O_2 at low overpotential.[14] Bearing this consideration in mind, we accordingly designed a new bio-inspired multicopper ORR catalyst in which a dinuclear Cu complex was immobilized on the surface of reduced graphene oxide (rGO) *via* the covalent grafted triazole-dipyridine (TADPy) dinucleating ligand

(Figure 1b). Adjacently arranged dinuclear Cu complexes on rGO may form multinuclear Cu centers, thus mimicking the active site of laccase. This rGO-TADPyCu composite showed excellent ORR activity and surprisingly high stability in alkaline media.

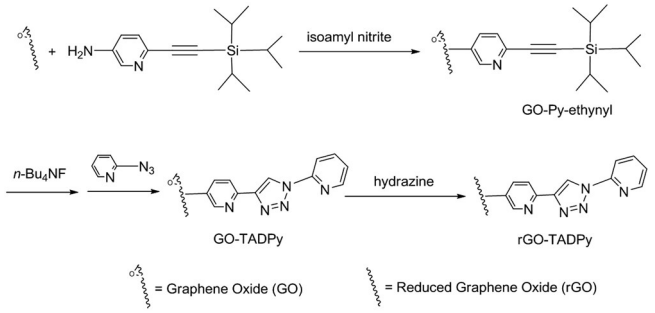

Scheme 1 Schematic route for the preparation of the rGO-TADPy

Due to its high specific surface area and high electrical conductivity, graphene has emerged as a promising support material for electrocatalysts.[15] In most cases, electrocatalysts were physically adsorbed on the surface of a graphene sheet, which improved the dispersibility of indissolvable catalysts such as Pt nanoparticles.[15] In this work, we chose the alternative method of direct functionalization of graphene with an ORR catalyst via covalent surface modification. This covalent immobilization approach may benefit from the facile electron transfer between the catalyst and the supporting material as well as from tightly holding the catalyst without detaching it from the support.

The preparation route for the covalent functionalization of graphene with TADPy is shown in Scheme 1. We employed *in situ* generation of an aryl diazonium for covalent functionalization of graphene oxide (GO) using isoamyl nitrite and pyridin-ethynyl-amine.[16] This reaction was evidenced by the FTIR spectrum of the GO-pyridin-ethynyl product where a prominent peak at 2198 cm^{-1} was assignable to the stretching vibration of the grafted pyridin-ethynyl groups (Figure 2a), which shifted from 2146 cm^{-1} in the pyridin-ethynyl-amine reactant (Figure S1). Grafting the TADPy ligand onto GO was then accomplished through a "click" reaction between the as-prepared GO-pyridin-ethynyl precursor and 2-azidopyridine. X-ray photoelectron spectroscopy (XPS) was used to verify the successful functionalization of GO with the TADPy ligand. The XPS survey spectrum of GO-TADPy showed the signatures of carbon, nitrogen, and oxygen (Figure 2c). The high resolution N1s XP spectrum of GO-TADPy revealed two nitrogen signals, which were deconvoluted into three components with binding energy (BE) of 399.3, 400.0, and 401.7 eV (Figure 2d). The peak at 399.3 eV can be assigned to the pyridine-N, and the peaks at 400.0 and 401.7 eV were then attributed to the triazole-N.[7a, 17a] The FTIR spectrum of GO-TADPy showed additional signals at 1100 and 1441 cm^{-1} when compared with that of GO (Figure 2a), which were assignable to stretching vibrations of the triazole ring.[7a, 17b] Accordingly, both the XPS analysis and the IR results suggested the presence of a triazole group, thus indicating successful formation of the TADPy ligand on GO.

The triazole-dipyridine functionalized graphene oxide, GO-TADPy, was subsequently subjected to hydrazine reduction to afford the reduced graphene oxide composite, rGO-TADPy. The high resolution XP C1s spectrum of rGO-TADPy displayed a significant decrease of the signals at 286–288 eV when compared with that of GO-TADPy (Figure 2f), suggesting the loss of surface C–O and C=O functionalities (Figure 2e).[16a] The oxygen atom content arising from surface oxygen groups in rGO-TADPy was reduced to ~12 at% compared with ~21 at% in GO-TADPy. This result indicated that chemical reduction of GO-TADPy by hydrazine resulted in significant removal of surface oxygen groups from GO, which restores the electrical conductivity of the chemically reduced graphene composite.

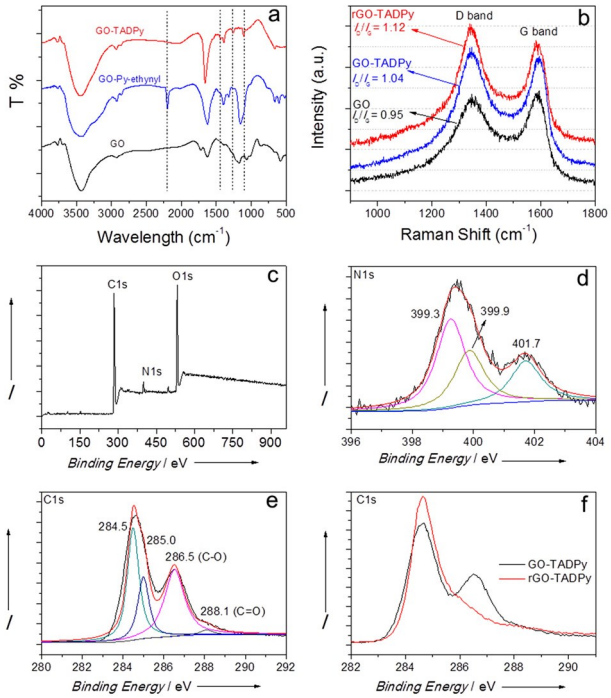

Figure 2 (a) FTIR spectra of GO (black), GO-py-ethynyl (blue) and GO-TADPy (red). (b) Raman spectra of GO (black), GO-TADPy (blue) and rGO-TADPy (red). Excitation = 532 nm. (c) XPS survey spectrum of GO-TADPy. (d) High resolution XP N1s spectrum of GO-TADPy. (e) High resolution XP C1s spectrum of GO-TADPy. (f) Comparison of high resolution XP C1s spectrum of GO-TADPy (black) and rGO-TADPy (red).

Raman spectroscopy was also used to probe the process of functionalization of GO. The Raman spectra of GO, GO-TADPy and rGO-TADPy in the high frequency region showed two peaks at 1340 and 1589 cm^{-1} (Figure 2b), which are normally referred to the D and G bands, respectively.[18] The D band is associated with the A_{1g} mode, which mainly arises from disorders and edges in graphite materials, while the G band corresponds to the symmetric E_{2g} mode, which originates from an in-plane sp^2 carbon–carbon double bond stretching motion.[18] The D/G band intensity ratio for rGO-TADPy (I_D/I_G = 1.12) was larger than those of GO-TADPy (I_D/I_G = 1.04) and GO (I_D/I_G = 0.95), which indicates that more defects were created on the surface of rGO after covalent grafting and reduction of GO. This phenomenon is due to the formation of new domains consisting of conjugated carbon atoms, as well as the increase of defect density after removal of oxygen functional groups, which is consistent with the previously reported rGO systems.[19].

Incorporation of copper ions in the TADPy functionalized rGO afforded the final catalyst rGO-TADPyCu composite, whose morphology was examined by transmission electron microscopy (TEM, Figure 3a) and atomic force microscopy (AFM, Figure S2). The TEM image of the rGO-TADPyCu composite showed small pieces of functionalized rGO with dimensions less than 50 nm × 50 nm. The elemental composition of rGO-TADPyCu was analyzed by XPS. The survey spectrum of rGO-TADPyCu showed the signatures of carbon, nitrogen, oxygen, chlorine, and copper (Figure 3b). The

copper content was determined to be 0.56 at%. The Cu2p core–level XP spectrum displayed two major peaks at 930–938 eV and 950–958 eV, which were assigned to the BE values of Cu2p3/2 and Cu2p1/2, respectively.[12d] Broad Cu(II) satellite peaks at 940–947 eV and 960–967 eV were noted (Figure 3c). The high resolution N1s XP spectrum of rGO-TADPyCu showed a broad nitrogen signal, which was deconvoluted into three components with binding energies of 399.0 eV, 400.0 eV and 401.0 eV (Figure 3d). After Cu incorporation, the binding energies assignable to the pyridine-N (399.0 eV) and the triazole-N (400.0, 401.0 eV) with the rGO-TADPyCu composite demonstrated up shifts when compared with those of the rGO-TADPy (pyridine-N: 398.3 eV; triazole-N: 399.3, 400.2 eV, Figure S3), suggesting the coordination of the TADPy ligand with Cu ions. The N-to-Cu ratio of 5.8 indicates the overall covalent attached TADPy ligands most probably coordinate with Cu ions in a 1:1 ratio as suggested in Figure 1b.

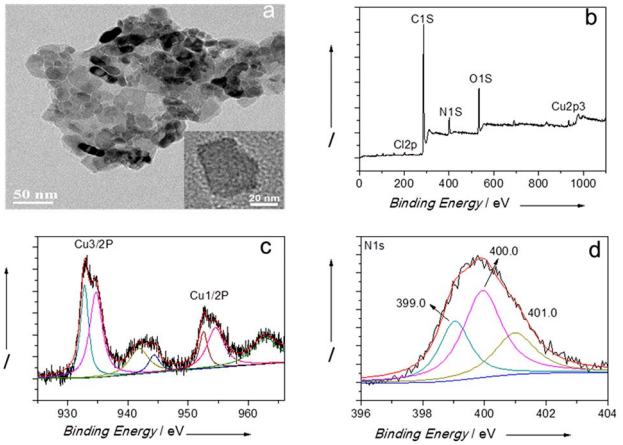

Figure 3 (a) TEM image of rGO-TADPyCu. Inset shows the high resolution TEM image. (b) XPS survey spectrum of rGO-TADPyCu. (c) High resolution XP Cu2P spectrum of rGO-TADPyCu. (d) High resolution XP N1s spectrum of rGO-TADPyCu.

Electrochemical characterization of rGO-TADPyCu as an ORR catalyst was then evaluated in an O_2-saturated 0.1M KOH solution using a rotating ring-disk electrode at room temperature. Cyclic voltammetry (CV) of rGO-TADPyCu in a 0.1M KOH solution revealed that in the absence of O_2, only a clean capacitive CV background was observed; however, the introduction of O_2 led to a large cathodic current with a peak at ~0.8 V vs. RHE (Figure 4a), indicating good O_2 catalytic activity of rGO-TADPyCu. Linear sweep voltammetry (LSV) was used to further evaluate the catalyst ORR performance. Physisorbed rGO/TAPyCu (a simple mixture of rGO and a mononuclear triazole-pyridine TAPyCu complex, Figure S4), and rGO/TADPyCu (a simple mixture of rGO and a dinuclear triazole-dipyridine TADPyCu complex, Figure S5), were used as control samples. The ORR polarization curves of the rGO-TADPyCu catalyst demonstrates both of an enhanced limit current density as well as onset potential (E_{onset}) relative to those of control samples (Figure 4b). The rGO-TADPyCu catalyst showed half-wave potential ($E_{1/2}$) value of 0.795 V vs. RHE at 1600 rpm. The E_{onset} (0.951 V, Figure 4c) with the rGO-TADPyCu catalyst showed significant positive shift compared with that of the metal-free rGO (E_{onset} = 0.887 V, Figure S6, S8), and it is also much more positive than that of the physisorbed mononuclear rGO/TAPyCu (E_{onset} = 0.917 V, Figure S6, S8) and dinuclear rGO/TADPyCu composite (E_{onset} = 0.937 V, Figure S7, S8). The onset potential is one of the important criteria used to evaluate the ORR activity of an electrocatalyst. These results indicated that a much lower ORR overpotential is observed with the rGO-TADPyCu catalyst when all the examined samples are compared. To the best of our knowledge, the $E_{1/2}$ value of 0.795 V and the E_{onset} of 0.951 V are the most positive ones among the Cu complexes as ORR catalysts reported to date.[11, 12]

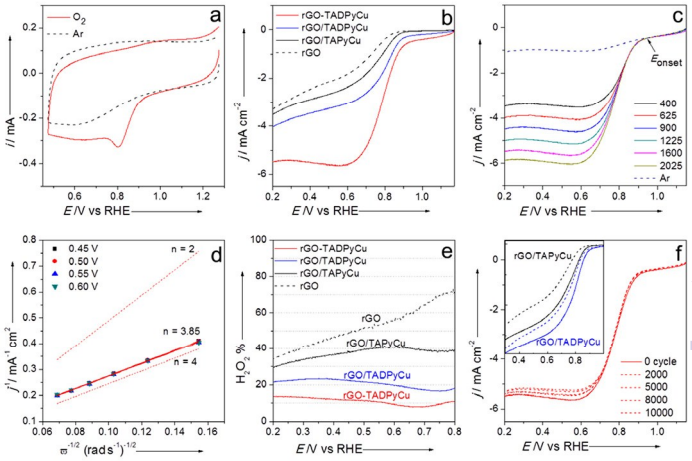

Figure 4 (a) Cyclic voltammograms of rGO-TADPyCu in Ar (dotted black) and O_2-saturated (red solid) 0.1 M KOH solution (b) Linear scanning voltammograms of rGO-TADPyCu (red), rGO/TADPyCu (blue), rGO/TAPyCu (black) and rGO (dashed black) catalysts in O_2-saturated 0.1 M KOH. Electrode rotation speed 1600 rpm; scan rate, 10 mVs^{-1}; loading, 0.6 mg cm^{-2}. (c) Rotating-disk voltammograms of rGO-TADPyCu in O_2-saturated 0.1 M KOH solution at the different rotation rates indicated. The dotted line indicates the background when scanned in Ar-saturated solution, loading 0.6 mg cm^{-2}. (d) Koutecky–Levich plots at different potentials. Scan rate, 10 mVs^{-1}. Theoretical $2e^-$ and $4e^-$ reduction processes are shown as dotted lines. (e) Peroxide yield for rGO-TADPyCu (red), rGO/TADPyCu (blue), rGO/TAPyCu (black) and rGO (dashed black) catalysts in O_2-saturated 0.1 M KOH. (f) ORR polarization plots of rGO-TADPyCu after 0, 2000, 5000, 8000, and 10,000 potential cycles in an O_2-saturated 0.1 M KOH solution, respectively. Inset shows ORR polarization plots of rGO/TADPy (blue) and rGO/TAPy (black) after 0 and 10,000 cycles, respectively. Potential was cycled between 0.575 and 0.975 V at a rate of 50 mVs^{-1}. Electrode rotation speed 1600 rpm.

The rotating-disk voltammograms of the rGO-TADPyCu catalyst at different rotation rates are shown in Figure 4c, and its rotation-rate-dependent current–potential curves are depicted in Figure 4d, where linear Koutecky–Levich plots were observed. The electron transfer number (n) was calculated to be 3.85 from the slopes of Koutecky–Levich plots at 0.45–0.60 V, suggesting a principal $4e^-$ oxygen reduction process. The amount of partially reduced product H_2O_2 detected from the ring electrode in the potential range from 0.6 V to 0.8 V was ~10%. However, within the same potential range, the amount of H_2O_2 increased to ~20%, ~40% and ≥60% with the rGO/TADPyCu, rGO/TAPyCu and rGO catalysts, respectively (Figure 4e). These results evidently suggested that the multinuclear Cu center within the rGO-TADPyCu catalyst is responsible for the high selectivity of $4e^-$ vs. $2e^-$ oxygen reduction. Furthermore, the rGO-TADPyCu catalyst catalyzes the ORR with less than 2% H_2O_2 generated in a phosphate buffer solution (pH 6.4, Figure S9).

Durability is also one of the major factors used to measure ORR performance in fuel cell technology. The stability of the rGO-TADPyCu catalyst was evaluated by an accelerated durability test protocol, in which the potential was cycled between 0.575 and 0.975 V at 50 mVs^{-1} in a 0.1M KOH solution saturated with O_2. A subtle negative shift of $E_{1/2}$ ($\Delta E_{1/2}$ ~-4 mV) was observed for the rGO-TADPyCu catalyst after 10,000 continuous cycles (Figure 4f), while for the physisorbed rGO/TAPyCu ($\Delta E_{1/2}$ ~-80 mV) and rGO/TADPyCu ($\Delta E_{1/2}$ ~-41 mV) samples, an obvious negative shift of the $E_{1/2}$ value was noted under the same experimental conditions (Figure 4f). The catalyst stability was also verified by repeated CV cycles (Figure S10). The high stability of this bio-inspired rGO-

TADPyCu catalyst probably comes from the low overpotential for the ORR and the high selectivity of 4e^- reduction process. Moreover, the covalent immobilization of the catalyst onto rGO also contributed beneficial effects. All these catalyst stability test results clearly confirm that the covalent grafted multinuclear Cu catalyst has excellent stability in alkaline media, which outperformed the other Cu ORR catalysts reported,[11-13] and is also superior to the Pt/C catalyst under similar conditions (Figure S11).

A methanol cross-over test on the rGO-TADPyCu catalyst was also performed. As is usual for non-precious-metal catalysts, the rGO-TADPyCu catalyst exhibited a stable amperometric response after the introduction of 2.0 M methanol, whereas the corresponding chronoamperometric response of the Pt/C catalyst displayed an abrupt decrease in the current upon the addition of 2.0 M methanol (Figure S11). These results suggest that the rGO-TADPyCu catalyst has a good tolerance to the methanol cross–over effect and may be used as a methanol–tolerant cathode catalyst in direct methanol fuel cells.

In summary, taking inspiration from the multicopper centers in the active site of laccase, we prepared a novel multicopper–graphene composite rGO-TADPyCu as an ORR catalyst, in which a dinuclear Cu complex was immobilized on the surface of rGO *via* the covalent grafted TADPy dinucleating ligand. This bio-inspired rGO-TADPyCu catalyst displayed a high selectivity of 4e^- reduction process compared with that of the physisorbed mononuclear rGO/TAPyCu as well as the dinuclear rGO/TADPyCu catalysts. The rGO-TADPyCu catalyst showed excellent stability and high ORR activity in alkaline media (E_{onset} = 0.951V vs. RHE), rendering it the hitherto most efficient Cu ORR catalyst reported. This work demonstrated that a covalent immobilization of bio-inspired multicopper model complex on carbon–based material is a promising approach for preparing a robust Cu ORR catalyst while mimicking the laccase catalytic ORR activity. This biomimetic rGO-TADPyCu catalyst may provide a hopeful alternative to noble metal catalysts in alkaline fuel cells.

This study was financially supported by the NSF of China (21271072), the Program for Professor of Special Appointment (Eastern Scholar) at the Shanghai Institutions of Higher Learning, and sponsored by the Shanghai Pujiang Program (13PJ1401900).

Notes and references

[a]*Key Laboratory for Advanced Materials of MOE & Department of Chemistry, East China University of Science and Technology, Shanghai, 200237, P. R. China, E-mail: liujingang@ecust.edu.cn*

†Electronic Supplementary Information (ESI) available: Experimental details and additional figures. See DOI: 10.1039/c000000x/

1 (a) M. K. Debe, Nature 2012, **486**, 43; (b) F. Y. Cheng, J. Chen, *Chem. Soc. Rev.* 2012, **41**, 2172; (c) R. Cao, J.-S. Lee, M. Liu, J. Cho, *Adv. Energ. Mater.* 2012, **2**, 816.

2 (a) S. Guo, S. Zhang, S. Sun, *Angew. Chem. Int. Ed.* 2013, **52**, 8526; (b) J. N. Tiwari, R. N. Tiwari, G. Singh, K. S. Kim, *Nano Energy* 2013, **2**, 553; (c) A. Morozan, B. Jousselme, S. Palacin, *Energy Environ. Sci.* 2011, **4**, 1238.

3 (a) Z. Chen, D. Higgins, A. Yu, L. Zhang, J. Zhang, *Energy Environ. Sci.* 2011, **4**, 3167; (b) R. Othman, A. L. Dicks, Z. Zhu, *Intl. J. Hydrogen Energy* 2012, **37**, 357.

4 (a) M. Lefèvre, E. Proietti, F. Jaouen, J.-P. Dodelet, *Science* 2009, **324**, 71; (b) G. Wu, K. L. More, C. M. Johnston, P. Zelenay, *Science* 2011, **332**, 443; (c) G. Wu, P. Zelenay, *Acc. Chem. Res.* 2013, **46**, 1878; (d) F. Jaouen, E. Proietti, M. Lefevre, R. Chenitz, J.-P. Dodelet, G. Wu, H. T. Chung, C. M. Johnstonb, P. Zelenay, *Energy Environ. Sci.* 2011, **4**, 114.

5 (a) A. Morozan, F. Jaouen, *Energy Environ. Sci.* 2012, **5**, 9269; (b) Y. Ren, G. H. Chia, Z. Gao, *Nano Today* 2013, **8**, 577.

6 (a) J. P. Collman, N. K. Devaraj, R. A. Decréau, Y. Yang, Y.-L. Yan, W. Ebina, T. A. Eberspacher, C. E. D. Chidsey, *Science* 2007, **315**, 1565; (b) M. S. Thorum, J. Yadav, A. A. Gewirth, *Angew. Chem. Int. Ed.* 2009, **48**, 165; (c) W. Li, A. Yu, D. C. Higgins, B. G. Llanos, Z. Chen, *J. Am. Chem. Soc.* 2010, **132**, 17056; (d) R. Cao, R. Thapa, H. Kim, X. Xu, M. G. Kim, Q. Li, N. Park, M. Liu, J. Cho, *Nat. Commun.* 2013, **4**, 2076.

7 (a) P.-J. Wei, G.-Q. Yu, Y. Naruta, J.-G. Liu, *Angew. Chem. Int. Ed.* 2014, **53**, 6659; (b) J.-G. Liu, Y. Naruta, F. Tani, *Angew. Chem. Int. Ed.* 2005, **44**, 1836; (c) J.-G. Liu, T. Ohta, Y. Yamaguchi, T. Ogura, S. Sakamoto, Y. Maeda, Y. Naruta, *Angew. Chem. Int. Ed.* 2009, **48**, 9262; (d) J.-G. Liu, Y. Shimizi, T. Ohta, Y. Naruta, *J. Am. Chem. Soc.* 2010, **132**, 3672; (e) T. Ohta, J.-G. Liu, Y. Naruta *Coord. Chem. Rev.* 2013, **257**, 407.

8 (a) K. D. Karlin, *Nature* 2010, **463**, 168; (b) M. T. Kieber-Emmons, M. F. Qayyum, Y. Li, Z. Halime, K. O. Hodgson, B. Hedman, K. D. Karlin, E. I. Solomon, *Angew. Chem. Int. Ed.* 2012, **51**, 168; (c) S. P. de Visser, J. S. Valentine, W. Nam, *Angew. Chem. Int. Ed.* 2010, **49**, 2099.

9 (a) L. M. Mirica, X. Ottenwaelder, T. D. P. Stack, Chem. Rev. 2004, **104**, 1013; (b) A. C. Rosenzweig, M. H. Sazinsky, Curr. Opin. Struc. Biol. 2006, **16**, 729.

10 (a) N. Mano, J. L. Fernandez, Y. Kim, W. Shin, A. J. Bard, A. Heller, *J. Am. Chem. Soc.* 2003, **125**, 15290; (b) J. A. Cracknell, K. A. Vincent, F. A. Armstrong, *Chem. Rev.* 2008, **108**, 2439.

11 (a) M. S. Thorum, J. Yadav, A. A. Gewirth, *Angew. Chem. Int. Ed.* 2009, **48**, 165; (b) F. R. Brushett, M. S. Thorum, N. S. Lioutas, M. S. Naughton, C. Toron, H.-R.M. Jhong, A. A. Gewirth, P. J. A. Kenis, *J. Am. Chem. Soc.* 2010, **132**, 12185; (c) M. A. Thorseth, C. E. Tornow, E. C. M. Tse, A. A. Gewirth, *Coord. Chem. Rev.* 2013, **257**, 130 and references cited therein; (d) E. C. M. Tse, D. Schilter, D. L. Gray, T. B. Rauchfuss, A. A. Gewirth, *Inorg. Chem.* 2014, **53**, 8505.

12 (a) Q. He, X. Yang, R. He, A. Bueno-Lopez, H. Miller, X. Ren, W. Yang, B. Koel, *J. Power Source* **2012**, 213, 169; (b) M. Jiang, L. Li, D. Zhu, H. Zhang, X. Zhao, *J. Mater. Chem. A* 2014, **2**, 5323; (c) M. Jahan, Z. Liu, K. P. Loh, *Adv. Funct. Mater.* 2013, **23**, 5363; (d) J. Mao, L. Yang, P. Yu, X. Wei, L. Mao, *Electrochem. Commun.* 2012, **19**, 29; (e) L. Ding, J. L. Qiao, X. F. Dai , J. Zhang, J. J. Zhang, B. L. Tian, *Int. J. Hydrogen Energy* 2012, **37**, 14103; (f) X. Qing, J. J. Shi, C. Y. Ma, M. Y. Fan, Z. Y. Bai, Z. W. Chen, J. L. Qiao, J. J. Zhang. *J. Power Sources.* 2014, **266**, 88.

13 Copper metal and copper oxide have also been explored as ORR catalyst. See: (a) C. O. Aniab, M. Seredycha, E. Rodriguez-Castellonc, T. J. Bandosz. *Appl. Catal., B: Environ.* 2015, **163**, 424; (b) R. F. Zhou, Y. Zheng, D. Hulicova-Jurcakovac, S. Z Qiao. *J. Mater. Chem. A.* 2013, **1**, 13179.

14 C. C. L. McCrory, A. Devadoss, X. Ottenwaelder, R. D. Lowe, T. D. P. Stack, C.E. D. Chidsey, *J. Am. Chem. Soc.* 2011, **133**, 3696.

15 (a) C. Zhu, S. Dong, *Nanoscale* 2013, **5**, 1753; (b) D. A. C. Brownson, D. K. Kampouis, C. E. Banks, *J. Power Source* 2011, **196**, 4873.

16 (a) Y. Zhu, A. L. Higginbotham, J. M. Tour, *Chem. Mater.* 2009, **21**, 5284; (b) C. K. Chua, M. Pumera, *Chem. Soc. Rev.* 2013, **42**, 3222.

17 (a) T. Palacin, H. L. Khanh, B. Jousselme, P. Jegou, A. Filoramo, C. Ehli, D. M. Guldi, S. Campidelli, *J. Am. Chem. Soc.* 2009, **131**, 15394; (b) H.-X. Wang, K.-G. Zhou, Y.-L. Xie, J. Zeng, N.-N. Chai, J. Li, H.-L. Zhang, *Chem. Commun.* 2011, **47**, 5747.

18 (a) L.M. Malard; M.A. Pimenta, G. Dresselhaus, M.S. Dresselhaus, *Phys. Rep.* 2009, **473**, 51; (b) M. A. Pimenta, G. Dresselhaus, M. S. Dresselhaus, L. G. Cancado, A. Jorio, R. Saito, *Phys. Chem. Chem. Phys.* 2007, **9**, 1276.

19 (a) H. Liu, L. Zhang, Y. Guo, C. Cheng, L. Yang, L. Jiang, G. Yu, W. Hu, Y. Liu, D. Zhu, *J. Mater. Chem. C* 2013, **1**, 3104; (b) H. Feng, R. Cheng, X. Zhao, X. Duan, J. Li, *Nat. Commun.* 2013, **4**, 1539; (c) A. Ganguly, S. Sharma, P. Papakonstantinou, J. Hamilton *J. Phys. Chem. C* 2011, **115**, 17009.

